Introduction of resonant states and enhancement of thermoelectric properties in half-Heusler alloys

J. W. Simonson,[1,*] D. Wu,[1] W. J. Xie,[2] T. M. Tritt,[2] and S. J. Poon[1]

[1]*Department of Physics, University of Virginia, 382 McCormick Rd., Charlottesville, Virginia 22904-4714, USA*

[2]*Department of Physics & Astronomy, Clemson University, 118 Kinard Laboratory, Clemson, South Carolina 29631-0978, USA*

(Received 19 October 2010; revised manuscript received 3 May 2011; published 29 June 2011)

The inclusion of small concentrations of vanadium (less than 1%) was found to produce a substantial increase in the Seebeck coefficient of polycrystalline *n*-type half-Heusler alloys based on $Hf_{0.75}Zr_{0.25}NiSn$. Some degree of vanadium-induced thermopower enhancement was found to be present even at temperatures as high as 800 K. Electrical resistivity values of the vanadium-doped samples, on the other hand, exhibited only modest increases, thereby resulting in a 120% increase in the thermoelectric power factor of $Hf_{0.75}Zr_{0.25}NiSn$ above room temperature. Such augmentation of the Seebeck coefficient, however, was diminished at all measured temperatures with the addition of a sufficient quantity of antimony to dope this class of compounds optimally. These observations are discussed in terms of carrier concentration, mobility, effective mass, and calculations of the effective gap size. When taken in conjunction with low temperature heat capacity measurements, these results indicate an increase in the density of states at the Fermi level that is consistent with the resonant state phenomena investigated earlier by theoretical work on semiconductors.

DOI: 10.1103/PhysRevB.83.235211 PACS number(s): 72.20.Pa, 72.15.Eb, 65.40.Ba

I. INTRODUCTION

Thermoelectric materials have been utilized for decades in niche applications such as electrical power generators on deep-space probes or as cooling units for computer chips and infrared sensors, but their widespread adoption has been hindered by their relatively low efficiency when compared with that of conventional compressor-based technologies. The thermoelectric efficiency is related to the dimensionless thermoelectric figure of merit, $ZT = \alpha^2\sigma T/\kappa$, where σ is the electrical conductivity, α is the Seebeck coefficient, and κ is the sum of lattice and electronic contributions to thermal conductivity. Despite the best efforts of researchers across several fields, the figure of merit of the most efficient bulk materials has remained around $ZT = 1$ for 50 years, largely due to the close interrelation of the relevant material properties involved. Since that time, much of the work on enhancing the thermoelectric efficiency has been focused on reducing κ_{lattice} through methods such as nanostructuring, alloy scattering, or the formation of composite materials. In recent years, however, the idea of maximizing the $\alpha^2\sigma T$ numerator of ZT via band structure engineering has gained a following, with one prominent suggestion being the introduction of resonant states near the Fermi energy of prospective thermoelectric materials for the purpose of increasing the Seebeck coefficient.

Mahan and Sofo were the first to predict from first-principles arguments that the highest ZT for a given material can be realized when the electronic density of states at the Fermi level most closely resembles a Dirac delta function, i.e., that a sharp, narrow peak lies near the chemical potential.[1] Since then, the idea of enhancing ZT by triggering the formation of sharp resonances at the Fermi level has been applied to several systems. One of the first publications to offer evidence of the appearance of resonant states in bulk compounds with thermoelectric application was a study of $AgPb_mSbTe_{2+m}$ ($m \geqslant 18$), in which the addition of a chainlike superlattice of silver and antimony atoms to the semiconductor PbTe was shown to introduce impurity-induced states near the bandgap.[2] Materials of this form have since become known as LAST (lead-antimony-silver-telluride) compounds. Specifically, the introduction of silver atoms was shown to create states at the top of the valence band, which not only were resonant with that band but also extended into the gap region, while the equivalent situation was found for antimony atoms and the PbTe conduction band. These resonances were shown to accompany a significant improvement of ZT. In a similar vein, *ab initio* calculations on indium-doped PbTe showed the appearance of a localized indium-induced peak within the gap and another below the valence band minimum.[3] Moreover, the introduction of 2% thallium to PbTe was reported to increase ZT by a factor of 2 at 800 K. In this case, a distortion in the density of states at the top of the valence band – as indicated by calculations of high effective mass and by heat capacity measurements – was again suggested to be the cause, although the precise origin of this distortion has yet to be determined.[4]

Within the last year, first-principles density functional theory calculations were performed on oxygen-doped ZnSe, predicting that the inclusion of "highly mismatched" isoelectronic impurities are likewise capable of creating a localized subband with high carrier effective mass in the density of states.[5] The formation of such a resonance above the conduction band minimum in the ZnSe system was shown to be a direct result of strong hybridization of the local impurity atomic levels with the band structure of the majority composition, in this case stemming from the substantial difference between the respective electronegativities of oxygen and selenium. According to this model, electron charge density is attracted toward and spatially localized around the oxygen atom impurities. In terms of thermoelectric properties, a substitution of 3.125% oxygen was predicted to improve the Seebeck coefficient by a factor of 30 and the thermoelectric power factor ($\alpha^2\sigma$) by a factor of 180 at room temperature, with these substantial enhancements owing to the creation of the localized impurity subband. A similar study predicted

 ©2011 American Physical Society

comparable results in GaAs with nitrogen substitutions. A nitrogen-induced peak was shown to grow in size and to shift in position below the conduction band edge with increased impurity concentration.[6]

Over the course of the last decade, half-Heusler alloys have generated considerable interest as potential thermoelectric materials at temperatures near or above 1000 K. This attention is in large part due to the high Seebeck coefficient, low electrical resistivity, and high degree of thermal stability often found in this class of compounds. Moreover, as a potential analogy to the work on PbTe and ZnSe, several studies have suggested that the introduction of nonisovalent transition-metal dopants into half-Heusler alloys may also result in the enhancement of the density of states near or within the bandgap. For example, self-consistent tight-binding linear muffin-tin orbital (TB-LMTO) calculations have predicted that a peak appears within the bandgap of semiconducting VFeSb, TiCoSb, and TiNiSn compounds when as little as 3.125% and as many as 25% of the atoms on the lower-valent transition-metal site are replaced with manganese, while substitution of transition metals to the other two sites was found to be energetically unfavorable.[7] Similar results were found with Korringa–Kohn–Rostoker (KKR) calculations performed with the coherent potential approximations (CPAs) and local density approximations (LDAs) on ZrNiSn with up to 10% cobalt doped to the nickel site, although no subsequent increase in *ZT* was reported.[8] More recently, a systematic study of gap size and thermoelectric properties has suggested a model for the location of dopant-induced peaks within the bandgap region in the case of 3d transition-metal substitution to either transition-metal site of $Hf_{0.75}Zr_{0.25}NiSn$.[9]

One of the central tenets put forth in each of these studies is that the bottom of the half-Heusler conduction band is dominated by states of the lower-valent transition metal, while the top of the valence band is mostly constructed of states from the higher-valent transition metal, as was first suggested several years ago.[10] The introduction of dopants that are located on the periodic table between these two extremes creates states near or within the gap and therefore near the Fermi energy. This argument is consistent with studies of scandium doping in TiNiSn,[11] yttrium doping in (Ti,Zr)NiSn,[12] and nickel doping in TiCoSb,[13] in which the dopant metal was located either to the left of the lower valent transition metal on the periodic table or to the right of the higher valent metal, and as a result no effects related to the introduction of an impurity peak were reported. In terms of studies of resonance phenomena in alloys within the Heusler family, however, very little work has been published to date. Recently, an *ab initio* study on the role of antisite defects in ZrNiSn was reported, finding a systematic shrinking of the gap with the number of defects as well as an enhancement of the density of states near the gap, enhancing *ZT* and prompting the authors to draw a comparison with the LAST system.[14] Very recent LDA calculations have also been performed on the full-Heusler compound Fe_2VAl, finding antisite disorder to introduce in-gap resonant states to the point of completely closing an indirect gap that the authors found to exist in the pristine compound to the detriment of the thermoelectric properties.[15] In the present paper, it is shown that small concentrations of vanadium substituted to the group IVB metal site of $Hf_{0.75}Zr_{0.25}NiSn$ have the effect of increasing the density of states at the Fermi level, thereby augmenting the thermoelectric properties of that compound at temperatures up to 650 K.

II. EXPERIMENTAL METHODS

Polycrystalline ingots of $(Hf_{0.75}Zr_{0.25})_{1-x}V_xNiSn$, where x was nominally equal to 0%, 0.25%, 0.5%, and 1%, were synthesized by arc melting elemental pieces under a flowing argon atmosphere. Additional ingots with 0% and 0.5% nominal vanadium concentrations were also each doped with 1% and 3% antimony to the tin site. The purity of each of the commercially obtained elements included in the melts was as follows: hafnium, 99.7%; zirconium, 99.95%; vanadium, 99.7%; nickel, 99.98%; tin, 99.99+%; antimony, 99.999%. Arc-melted ingots were flipped and remelted four times to ensure the homogeneity of the melt, and losses were strictly confined to less than 0.5% of the starting mass. Prior to measurement, all ingots were wrapped in tantalum foil, sealed in quartz ampoules under a pressure of less than 10 mTorr, and annealed at 900°C for 24 h followed by 800°C for 7 days. Ingots were polished after annealing to remove any surface contamination that may have been acquired during heat treatment. Phase purity was confirmed with powder x-ray diffraction (XRD) of Cu-Kα radiation over a 2θ range from 20° to 80°. Rietveld refinement of the diffraction data was performed with the GSAS/EXPGUI software package, revision 1.80.[16,17] Slices of the ingots were polished with SiC paper and fine-grain Al_2O_3 suspensions in water and were etched with a solution of acetic, nitric, and hydrofluoric acids. Etched slices were then viewed under an optical microscope and a scanning electron microscope (SEM) in order to image the microstructure. Energy-dispersive spectroscopy (EDS) line scans were performed to provide a qualitative picture of the distribution of the constituent elements throughout the microstructure. After annealing and measurement, the difference between nominal and actual ingot concentrations was determined with electron probe micro-analysis (EPMA).

Measurements of electrical resistivity and the Seebeck coefficient were carried out simultaneously from room temperature to 1100 K on a custom apparatus that has been described previously[18] and were performed during both the heating and cooling cycles. Electrical resistivity values varied less than approximately 1% from heating to cooling cycle, while Seebeck coefficient measurements of the different cycles were consistent to within 5% of one another. The larger discrepancy in the Seebeck coefficient measurement was observed to be due to degradation of the thermal contact between the sample and thermocouples upon cooling as a result of differential thermal expansion and contraction. Accordingly, repeated measurements of the same sample yielded thermopower measurements that were consistent to within 2.5%, indicating that the samples – which had previously been annealed – underwent no further heat treatment during the measurement cycles. Sample oxidation during measurement was observed to be minimal, as was expected given that the high-temperature apparatus was subjected to constant evacuation during measurement and that the measurement time period was limited to several hours. Any oxidation that did occur was observed as a mild tarnish

restricted to the surface of the sample that did not penetrate either the electrical or thermal junctions with the measurement apparatus, mitigating any effect on the observed properties.

Hall effect measurements were performed at room temperature on a quantum design physical properties measurement system (PPMS) using an AC transport (ACT) option in the five-wire configuration. Heat capacity measurements were performed on the same instrument in the low-temperature Debye regime, specifically from 1.8 to 5 K.

III. CALCULATIONS

The heat capacity data were observed to obey the following standard relation, allowing calculation of the density of states at the Fermi energy from the electronic specific heat term:

$$C_p = \gamma T + \beta T^3, \tag{1}$$

where

$$\gamma = \frac{\pi^2}{3} k_B^2 N(E_F). \tag{2}$$

The remaining calculations followed similar customary techniques. Carrier concentration was calculated from the slope of Hall resistivity vs applied magnetic field curves, assuming a single-band model. Carrier mobility, under the same set of assumptions, was calculated from the carrier concentration and the measured electrical conductivity at room temperature. A well-known method was utilized to calculate carrier effective mass, assuming a single parabolic band in which the dominant mechanism of carrier scattering is via longitudinal acoustic collisions with phonons ($r = 0$).[19] Accordingly, the reduced Fermi energy (η^*) was first calculated from the Seebeck coefficient at room temperature:

$$\alpha = \pm \frac{k_B}{e} \left(\frac{(2+r)F_{1+r}(\eta^*)}{(1+r)F_r(\eta^*)} - \eta^* \right), \tag{3}$$

where F_p is a Fermi integral of the order of p and is defined as

$$F_p(\eta^*) = \int_0^\infty \frac{x^p}{1+\exp(x-\eta^*)} dx. \tag{4}$$

The effective mass was then calculated from the carrier concentration and the reduced Fermi energy according to the expression

$$n = 4\pi \left(\frac{2m^* k_B T}{h^2} \right)^{3/2} F_{1/2}(\eta^*). \tag{5}$$

For nonzero values of p, no analytical solution to the Fermi integral exists, prompting the generation of numerical solutions with the Maple 13 program from Waterloo Maple.

The use of a single-band model for the above analysis was justified by the examination of so-called Jonker plots constructed with the temperature-dependent thermopower plotted against the electrical resistivity of the material measured at the same temperature.[20] In this manner, the Seebeck coefficient of a nondegenerate semiconductor can be fitted as a function of resistivity according to the expression

$$|\alpha| = c \frac{b-1}{b+1} \log_{10}(\rho) + d, \tag{6}$$

where

$$c = \frac{k_B}{e \log_{10} e} \cong 198\ \mu\text{V/K}, \tag{7}$$

$$d = \frac{k_B}{e} \left[\frac{b-1}{b+1} \ln\left(\frac{1}{\rho_0}\right) + \frac{3}{4} \ln\left(\frac{m_h}{m_e}\right) + \frac{bA_h - A_e}{b+1} \right], \tag{8}$$

in which ρ_0 is the scaling term from the activated behavior of the electrical resistivity; m_h and m_e are the hole and electron effective masses, respectively; and A_h and A_e are the hole and electron transport parameters. The parameter b is a ratio of the electron and hole mobilities and concentrations:

$$b = \frac{n_e \mu_e}{n_h \mu_h}. \tag{9}$$

For the undoped material, as well as the compounds doped with 0.25% and 0.5% vanadium, the calculated b parameter varied from 7.1 to 7.4, indicating that in each of these systems the mobility of the majority carrier was significantly greater than that of the minority carrier and that the transport can be well approximated by a single-band model.[21] The b parameter for the 1% vanadium doped was only 3.6 – somewhat smaller than was the case for samples with lower vanadium concentrations but nonetheless indicative of the significant dominance of n-type transport.

IV. RESULTS AND DISCUSSION

A. Phase and compositional analysis

Composition analysis was performed by EPMA after both heat treatment and high-temperature measurements had been completed. The following compositions were determined: $Hf_{0.75}Zr_{0.25}Ni_{1.0}Sn_{0.99}$ for the undoped compound, with the vanadium concentration of that ingot falling below the 50-ppm detection limit; $Hf_{0.75}Zr_{0.25}V_{0.0024}Ni_{1.0}Sn_{1.0}$ for the nominally 0.25% doped sample; $Hf_{0.75}Zr_{0.25}V_{0.0063}Ni_{1.0}Sn_{0.99}$ for the nominally 0.5% doped sample; and $Hf_{0.73}Zr_{0.27}V_{0.0078}Ni_{0.99}Sn_{1.0}$ for the nominally 1% doped compound. For all samples tested, antimony was not observed above the 200-ppm detection limit, as was expected. Two somewhat significant discrepancies from the nominal compositions, however, were observed in the two ingots containing the highest vanadium concentrations. First, the vanadium concentration of the nominally 0.5% alloy was somewhat higher than expected, while the concentration of the 1% alloy was somewhat lower. These measured vanadium concentrations appear throughout the remainder of this paper in place of the nominal concentrations. Second, the Hf-Zr ratio of the most heavily doped ingot is slightly different than that of the others. The impact of this difference on transport properties is expected to be minimal, given that hafnium and zirconium are isoelectronic and the discrepancy is small. Isoelectronic substitution of the lower valent transition-metal species has been studied for many years in TiNiSn-type compounds and has been used to optimize ZT in this class of materials via the introduction of alloy scattering. Such optimization, however, occurs typically over compositional ranges of tens of percents, suggesting a negligible impact of the 2% discrepancy observed in this study.[22]

Figure 1(a) displays the room-temperature powder XRD pattern of the most heavily vanadium-doped compound –

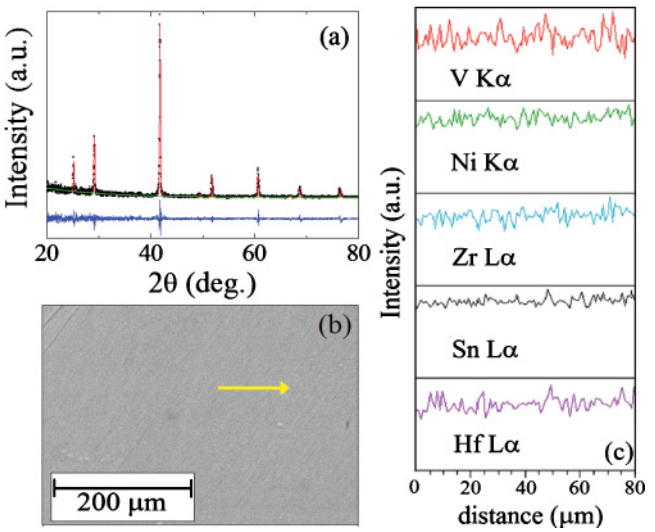

FIG. 1. (Color online) (a) Powder XRD scan of $(Hf_{0.75}Zr_{0.25})_{0.99}V_{0.0078}NiSn$ (black dots), Rietveld refinement (red line), background refinement (green line), and (observed – calculated) difference plot (blue line); (b) electron micrograph of the same sample; (c) EDS line scans collected over region indicated by yellow arrow.

i.e., 0.78% vanadium – along with the results of a Rietveld refinement and a plot of the difference between the observed and calculated patterns, which is drawn on the same scale. The refinement accounts for all peaks of the half-Heusler crystal structure, confirming the successful formation of the desired structure. Moreover, no peaks of a second phase were observed within the detection limit of the diffractometer, suggesting that the vanadium atoms were successfully incorporated into the host lattice. Furthermore, SEM micrographs conducted over multiple wide areas of the two most heavily vanadium-doped samples show no evidence of a second phase. No evidence of significant cracking or other microstructural defects was observed in the microstructure of the ingots under either the optical microscope or the SEM. An example micrograph is shown in Fig. 1(b) with the path of an EDS line scan some 80 μm in length demarcated by a yellow arrow. The corresponding line scan is presented in Fig. 1(c) and displays a uniform distribution of vanadium throughout the microstructure. Further, there is no evidence of phase segregation into multiple MNiSn half-Heusler regions with compositionally segregated hafnium, zirconium, and vanadium species, such as may not have been detected by XRD.

B. Thermoelectric properties of V-doped $Hf_{0.75}Zr_{0.25}NiSn$

Measurements of Seebeck coefficient, electrical resistivity, and thermoelectric power factor from room temperature to 1100 K are shown in Fig. 2. It can be seen from the upper two plots that a peak centered at 480 K appears in the thermopower measurements as vanadium atoms are substituted to the hafnium–zirconium site of the lattice. With only 0.24% vanadium substitution, the Seebeck coefficient is enhanced from -196 to -232 μV/K. Greater enhancement is achieved with 0.63% substitution to a maximum value of $-$ 260 μV/K before declining with further doping to -250 μV/ K at 1% V. In the maximal case of 0.63% doping, the enhancement persists until 760 K, whereupon the Seebeck coefficient of the vanadium-free compound reemerges as the highest of the compositions surveyed. In fact, at temperatures greater than about 800 K, it is observed that the Seebeck coefficients of the vanadium-doped compounds – particularly those with concentrations of 0.63% and higher – show a marked decline, culminating in a relative reduction of 39% at 1050 K with 0.78% vanadium substitution. In contrast, the electrical resistivity measurements carried out in tandem show little response to vanadium doping, despite the additional electrons contributed to the system via the inclusion of the higher-valent transition-metal atoms. That the electrical resistivity did not decrease with the addition of vanadium provides further evidence that that species was successfully integrated into the half-Heusler structure and was not distributed as a second metallic phase throughout the microstructure. Consequently, the thermoelectric power factor was enhanced at the lower end

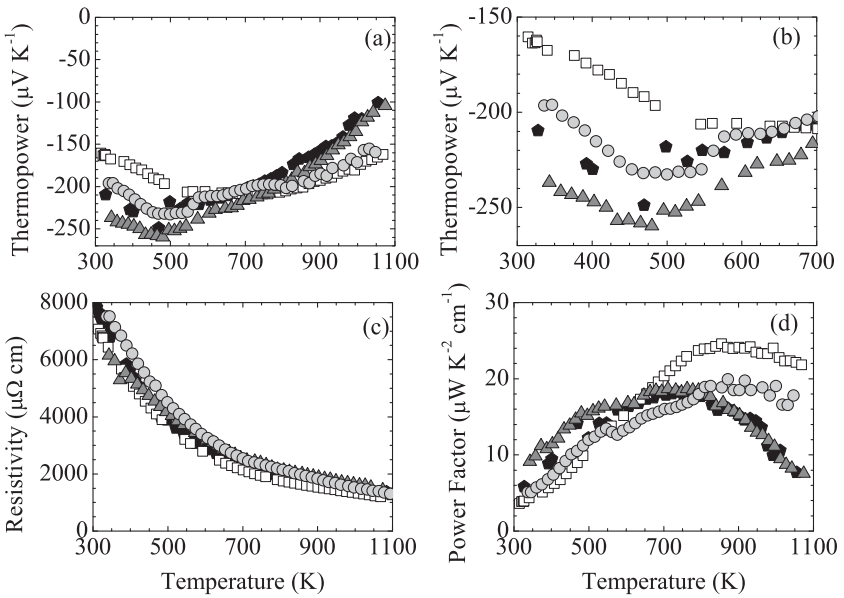

FIG. 2. (a),(b) High-temperature thermopower, (c), electrical resistivity, and (d) power factor (d) of $(Hf_{0.75}Zr_{0.25})_{1-x}V_xNiSn$, where $x = 0$ (white squares), 0.0024 (light-gray circles), 0.0063 (dark-gray triangles), and 0.0078 (black pentagons).

of the measured temperature spectrum and was diminished at higher temperatures. In particular, the compound with 0.63% vanadium showed an enhancement in the power factor up to 650 K and a maximum relative enhancement over the undoped compound of 120% at 380 K.

As has been proposed before,[7,9] these results suggest that the doping of transition metals into half-Heusler systems introduces a local feature in the density of states near to or within the bandgap region. This addition of impurity-induced states near the Fermi energy contributes toward a greater Seebeck coefficient at room temperature, while at higher temperatures *n*-type carriers are promoted into the conduction band, away from the local enhancement and therefore minimizing its benefit. What is more, at these temperatures the additional disorder imparted to the system by the inclusion of vanadium atoms into the lattice acts as an overall detriment to thermoelectric efficiency. The observation that such a relatively small concentration of vanadium impurity produced such a dramatic improvement of the Seebeck coefficient while leaving the electrical resistivity unchanged is consistent with recent reports of predicted resonant state behavior in the ZnSe and Ag-Pb-Sb-Te systems.[2,5] The case of the 0.24% vanadium-doped material may be considered here as an example. While the Seebeck coefficient of this compound is improved by a factor of nearly 20% by 450 K as a result of doping, no effects of this enhancement are present in measurements taken at temperatures of 600 K or higher, suggesting that, while the density of states is significantly altered at or near the Fermi energy, this modification is relevant across only a narrow energy scale – of the order of 50 meV, which is small compared with both the calculated 0.5-eV and measured 0.22-eV bandgaps.[9] Hence it appears that the resonance in lightly vanadium-doped $Hf_{0.75}Zr_{0.25}NiSn$ is qualitatively similar to Mahan and Sofo's Dirac function resonance and thus is remarkably distinct from the gap-spanning dopant-induced peaks predicted to form in half-Heusler compounds by *ab initio* calculations that considered significantly larger concentrations of manganese and cobalt dopant atoms.[7,8] In these cases, the resonance broadens with greater dopant concentration to the rapid detriment of thermoelectric properties and the consequent increase of disorder and of carrier scattering.[9] This interpretation is in accord with resistivity measurements as well in that no substantial decrease of that resistance was observed as might be expected if a broad gap state exhibited some degree of overlap with either the valence or conduction band of the bulk material.

In studies of resonant states in chalcogenide systems, it has been reported that the incorporation of a resonance into the density of states near the Fermi level coincided with a systematic decrease in the size of the bandgap. To extend the investigation of resonant state phenomena in half-Heusler compounds, an estimate of the bandgap was performed for each of the vanadium-doped compositions. To this end, a subset from 900 to 1030 K of the high-temperature electrical resistivity data for each of these compounds is presented in Fig. 3. The axes of the plot, $2k_B \ln(\rho)$ vs. $1/T$, were selected so that the size of the semiconducting gap of these materials could be determined from the slope of the resulting linear curves. Half-Heusler alloys have previously been shown to exhibit activated behavior in the intrinsic semiconductor regime at these sufficiently high temperatures.[23] Figure 3 illustrates that for compounds of the form $(Hf_{0.75}Zr_{0.25})_{1-x}V_xNiSn$ (x = 0%, 0.63%, and 0.78%), the slope of the lines is invariably equal to 0.22 eV, implying that there is no change in gap size, despite the addition of vanadium as a dopant. On the other hand, the 0.24% vanadium-doped curve indicates a slight expansion of the bandgap to 0.27 eV, in direct contrast to the behavior reported for the oxygen-doped ZnSe[5] and LAST[2] systems. These results also differ from the results of *ab initio* calculations finding the gap size in the Heusler compound Fe_2VAl to decrease to zero with the presence of defects and the subsequent onset of resonant states within the gap, suggesting a subtle difference behind any modification of the density of states of $(Hf_{0.75}Zr_{0.25})_{1-x}V_xNiSn$[15] For completeness, the measured values of the effective gap size of the vanadium-doped half-Heusler compounds are also included as entries in Table I.

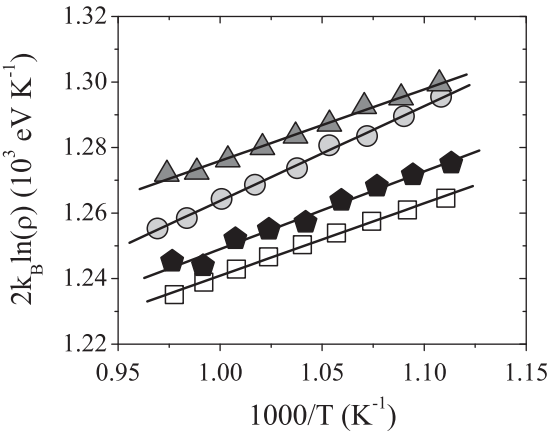

FIG. 3. Plots of $2k_B \ln(\rho)$ to display activated behavior in $(Hf_{0.75}Zr_{0.25})_{1-x}V_xNiSn$, where $x = 0$ (white squares), 0.0024 (light-gray circles), 0.0063 (dark-gray triangles), and 0.0078 (black pentagons) over the temperature range 900–1030 K. The lines connecting the points are lines of best fit determined by linear regression.

A recent letter provides a likely explanation for the relatively small change of the effective gap size with vanadium doping.[14] The results of *ab initio* calculations suggest that, even in undoped ZrNiSn, there exists a low but nonzero density of states within the gap due to antisite disorder, which pulls the Fermi energy up from the top of the valence band toward the middle of the gap. Furthermore, dopant-induced pinning or saturation of the Fermi energy akin to the above observations has been reported previously in transition-metal-doped half-Heusler compounds.[7–9] This phenomenon can be explained as a direct effect of the hybridization of an unstable vanadium *d* resonance into a stable electronic state capable of holding some number of electrons – depending on impurity concentration and degree of *d*-orbital hybridization– and thereby preventing the Fermi energy from reaching the majority conduction band until these resonant levels are overfilled by electrons contributed by another dopant, such as antimony. The saturation phenomenon was previously predicted and was described in detail by early theoretical work on impurity-induced resonant states in II-VI semiconductors, in particular for indium-doped PbTe.[24]

TABLE I. Thermopower enhancement and electronic properties of $(Hf_{0.75}Zr_{0.25})_{1-x}V_xNiSn$

x	S_{RT} (μV/K)	E_{gap}(eV)	n(cm^{-3})	μ (cm^2/ V s)	m^* (m_0)	γ (mJ/mol·K^2)	$N(E_F)$ (states/eV unit cell)	θ_D (K)
0	−167	0.22	5.5×10^{19}	16	1.5	0.42	2.2	250
0.0024	−196	0.27	4.2×10^{19}	20	1.6	0.49	2.5	250
0.0063	−237	0.22	4.1×10^{19}	24	2.2	0.53	2.7	252
0.0078	−209	0.22	3.3×10^{19}	25	2.1	0.78	4.0	251

C. Properties of carriers and electronic structure of V-doped $Hf_{0.75}Zr_{0.25}NiSn$

Figure 4 displays a comparison of the trend of enhancement in the room-temperature Seebeck coefficient with carrier properties that were calculated from thermoelectric and Hall measurements. Carrier concentration, mobility, effective mass, and the absolute value of the thermopower at room temperature are plotted on separate vertical axes as the concentration of vanadium is increased from 0% to 0.78%. While the room-temperature Seebeck coefficient reaches a maximum value of -237 μV/K with 0.63% vanadium doping, the carrier concentration systematically decreases by nearly a factor of two from 5.5×10^{19} to 3.3×10^{19} cm^{-3} as the vanadium concentration is varied from 0% to 0.78%. Because the electrical resistivity of this series of materials is nearly constant with respect to impurity concentration, however, this decrease in carrier concentration is complemented by an equally systematic increase in mobility from 16 to 25 cm^2/V s over the same range of vanadium doping. Meanwhile, the effective mass mirrors the Seebeck coefficient, increasing from 1.5 m_0 when no vanadium is present to 2.2 m_0 at the 0.63% level before rolling over with further doping. It is worth noting that the calculated values of carrier concentration, mobility, and effective mass for undoped $Hf_{0.75}Zr_{0.25}NiSn$ are consistent with those previously published in the literature for similar half-Heusler compositions,[25] whereas corresponding results have not been published on vanadium-doped compounds.

Overall, these regular trends in carrier behavior point to a substantial and systematic modification of the density of states near the Fermi energy with vanadium doping. For instance, that the carrier concentration of intrinsically n-type $Hf_{0.75}Zr_{0.25}NiSn$ is reduced instead of augmented by the surplus electrons donated by vanadium atoms is a strong indication that impurity-induced states have been added at or below the Fermi level. Less surprising, on the other hand, is the resultant increase in Seebeck coefficient with decreased carrier concentration as was predicted by very early work in the field.[26] In particular, the dependence of the Seebeck coefficient upon carrier concentration and mobility in thermoelectric systems with distorted band structures has been discussed in light of the Mott relation:[4,27]

$$\alpha \propto \frac{d}{dE}\ln\sigma = -e\frac{d}{dE}\ln[\mu \cdot n] = -\frac{e}{\mu}\frac{d\mu}{dE} - \frac{e}{n}\frac{dn}{dE}. \quad (10)$$

In the case of the $Hf_{0.75}Zr_{0.25}NiSn$ alloys, vanadium doping serves to supplement the number of valence electrons donated to the system, thereby increasing its energy. Qualitatively then, the Mott expression can be discussed in terms of derivatives that are taken with respect to vanadium concentration instead of with respect to energy. From Fig. 4, it is clear that the derivative of carrier concentration with respect to vanadium doping is uniformly negative, resulting in an overall positive value for the second term of the Mott relation. The resulting implication is that the enhancement in the n-type Seebeck coefficient in these compounds is driven by the increased carrier mobility. Once the slope of carrier mobility versus vanadium concentration begins to flatten at concentrations greater than 0.63% vanadium, however, the negative trend in carrier concentration dominates the relation, resulting in a relatively diminished Seebeck coefficient in the compound with 1% vanadium. The enhancement of the Seebeck coefficient and the density of states can also be thought of in terms of the effective mass, which is shown to be enhanced by a factor of 50% with vanadium doping. Simultaneous increase of carrier mobility and effective mass with doping is somewhat atypical, although not unprecedented when doping concentration is sufficiently small. Previous studies of resonant systems have explained observations of increased mobility with dopant concentration as indicative of the dominance of interimpurity Coulombic interactions over impurity-host hybridization, particularly when the Fermi energy is pinned by the impurity state.[28,29] Such an arrangement has the effect of minimizing impurity scattering.

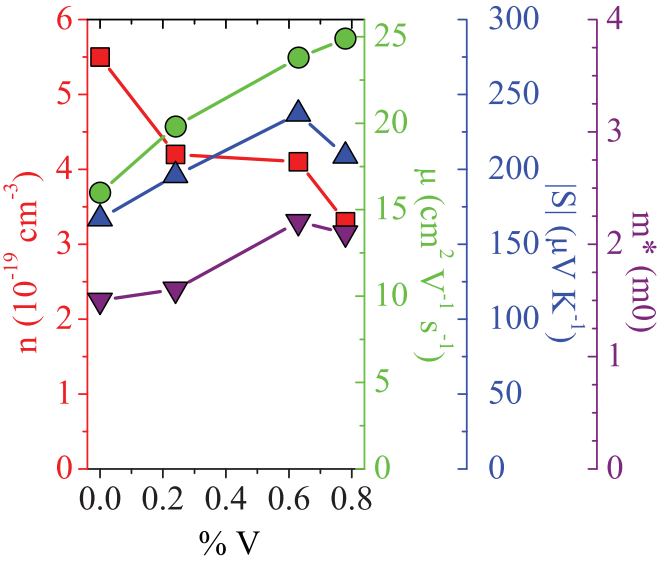

FIG. 4. (Color online) An overlay of plots of carrier concentration (left axis, red squares), carrier mobility (first right axis, green circles), absolute value of Seebeck coefficient (second right axis, blue upward triangles), and carrier effective mass (third right axis, purple downward triangles) of V-doped $Hf_{0.75}Zr_{0.25}NiSn$ as a function of V concentration. All values were measured at room temperature or calculated from room-temperature data.

Indeed the predicted formation via interimpurity interactions of a sort of superlattice of resonant ions is remarkable similar to the description of the LAST system and points to a substantial modification of the density of states.[2] Meanwhile, the narrow band dispersion of the resonance itself drives the effective mass to a higher value. The onset of this sharp modification to the band structure by necessity calls into question the assumption invoked in calculating the effective mass, i.e., of a parabolic band model. Such a simple model is likely unable to account for the substantial nonparabolic distortion of the density of states that appears to be introduced with greater degrees of vanadium substitution. In light of this development, heat capacity measurements were performed in order to offer a more direct view of modifications to the electronic structure at the Fermi level.

Indeed, further evidence for an increase in the density of states at the Fermi level is observed in the results of heat capacity measurements performed on vanadium-doped $Hf_{0.75}Zr_{0.25}NiSn$, as is displayed in Fig. 5. At temperatures less than 5 K, the conditions for the Debye regime are seen to be satisfied, resulting in linear behavior when C_P/T is plotted against T^2. As the vanadium concentration is varied from 0% to 0.78%, a systematic increase in the Sommerfeld constant from 0.42 to nearly 0.78 mJ/mol K^2 is observed, indicating a corresponding enhancement of the zero-temperature electronic density of states at the Fermi level from 2.2 to 4.0 states/eV per unit cell. Meanwhile, despite this nearly factor-of-two increase in γ, the Debye term of the heat capacity, which is given by the slope β, remains constant to within 2%–3%. The estimated Debye temperatures of the investigated compounds are presented in Table I and stand in good agreement with previous reports for undoped HfNiSn.[30] That they are constant to within 2 K with respect to vanadium concentration is

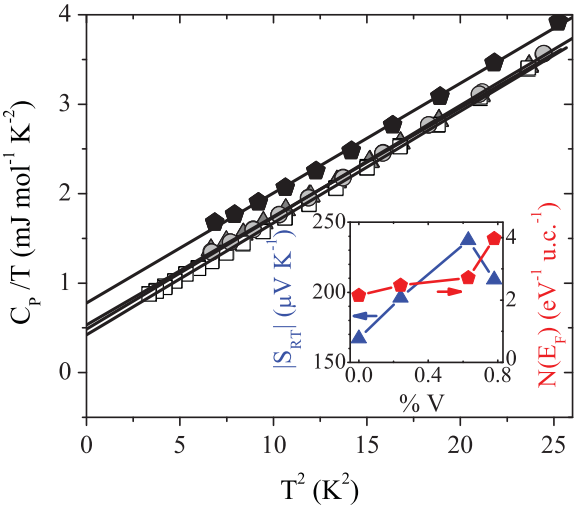

FIG. 5. (Color online) Heat capacity measurements of $(Hf_{0.75}Zr_{0.25})_{1-x}V_xNiSn$, where $x = 0$ (white squares), 0.0024 (light-gray circles), 0.0063 (dark-gray triangles), and 0.0078 (black pentagons) over the temperature range 1.8–5.0 K. The lines connecting the points are lines of best fit determined by linear regression. Inset: Absolute value of room-temperature Seebeck coefficient (left axis, blue triangles) and density of states at the Fermi level (right axis, red pentagons) plotted against vanadium concentration.

suggestive that the phonon spectrum is virtually unaffected by the introduction of vanadium to the lattice. This result is expected because such relatively small amounts of vanadium doping would be unlikely to result in a large change to the heat capacity of the lattice. In the inset of Fig. 5, the absolute value of the Seebeck coefficient at room temperature is plotted on the same axis as the density of states at the Fermi level for purposes of comparison, and likewise values of γ and $N(E_F)$ are tabulated in Table I. An inconsistency in the data set for the composition with 0.78% vanadium bears further consideration. The leveling off of the effective mass with increased vanadium concentration stands in contrast to the continued escalation of the Sommerfeld constant under the same circumstances. As discussed above, this disagreement may be a result of the assumption of a parabolic band model to determine the effective mass. Furthermore, as was revealed in the Jonker analysis discussed in the previous section, the single-band semiconductor model is able to provide a somewhat less accurate approximation of the 0.78% doped compound. A consistent explanation for the discrepancy is that the Seebeck coefficient begins to fall at higher levels of doping as the deformation of the electronic structure near the gap leads to increased lattice disorder or more likely as the impurity-induced peak broadens and overlaps with the conduction band, resulting in the onset of some degree of carrier compensation.

D. Thermoelectric properties of antimony-doped $(Hf_{0.75}Zr_{0.25})_{0.995}V_{0.005}NiSn$

Half-Heusler compounds such as $Hf_{0.75}Zr_{0.25}NiSn$ and $Hf_{0.50}Zr_{0.50}CoSb$ typically require some degree of doping with *p*-band elements to achieve high *ZT* at temperatures near 1000 K.[18,31] Hence, given the superior Seebeck coefficients measured in the vanadium-substituted compounds, it was deemed desirable to investigate the effects of antimony doping on these materials. These properties appear in Fig. 6. When 1% antimony was added to $(Hf_{0.75}Zr_{0.25})_{0.995}V_{0.005}NiSn$, the Seebeck coefficient was enhanced over a broad temperature range spanning from room temperature to nearly 850 K. At the same time, a small increase in electrical resistivity was measured, which was likely due to the increased electron scattering associated with the somewhat undersized vanadium impurities and the strain these size effects impart to the lattice. Hall measurements confirm that antimony indeed acts as a classical electron donor even in vanadium-doped compounds, with carrier concentration increasing from 4.1×10^{19} cm^{-3} in $(Hf_{0.75}Zr_{0.25})_{0.995}V_{0.005}NiSn$ to 3.5×10^{20} cm^{-3} in $(Hf_{0.75}Zr_{0.25})_{0.995}V_{0.005}NiSn_{0.99}Sb_{0.01}$, as is to be expected. In the case of an additional 2% antimony doping, no augmentation of the Seebeck coefficient was observed at any temperature, and indeed the thermopower was slightly diminished across the entire temperature spectrum. This lack of an enhancement was accompanied by an increase in the electrical resistivity by a factor of two, again across the entire temperature spectrum. As a result, while the thermoelectric power factor of the 1% antimony-doped compound was enhanced from room temperature to 800 K, power factor was approximately halved with 3% antimony doping at all temperatures measured.

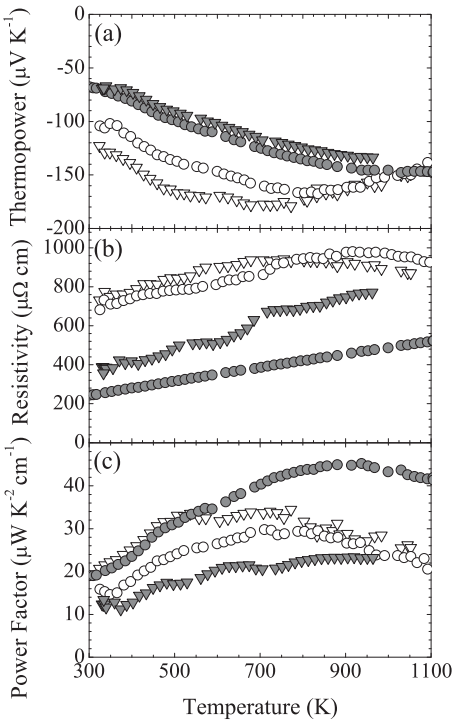

FIG. 6. (a) High-temperature thermopower, (b) electrical resistivity, and (c) power factor of $Hf_{0.75}Zr_{0.25}NiSn$ with 0% V and 1% Sb (white circles), 0.5% V and 1% Sb (white triangles), 0% V and 3% Sb (gray circles), and 0.5% V and 3% Sb (gray triangles).

Both the enhancement in thermopower and the slight increase in electrical resistivity in $(Hf_{0.75}Zr_{0.25})_{0.995}V_{0.005}NiSn_{0.99}Sb_{0.01}$ are expected to have much the same origin as those of the materials in which the tin site is undoped – the Seebeck coefficient is likely enhanced by a resonance in the density of states. At higher temperatures, however, the chemical potential is raised, and electrons are thermally promoted to the conduction band, in effect bypassing any influence from the localized resonance. A similar scenario arises with the addition of a greater degree of antimony, only in this case the chemical potential is raised not by temperature but by dopant concentration. In either case, the beneficial effects of the resonance are not observed, but the associated disorder introduced to the lattice and to the electronic structure result in an overall degradation of thermoelectric properties. Accordingly, it was decided not to pursue thermal conductivity measurements on these materials, given that any power factor enhancement with vanadium substitution in the antimony-doped compounds was either limited to low temperatures in the case of 1% doping or even completely absent in the case of 3% doping. Furthermore, it is considered unlikely that such a small substitution of vanadium would have any major effect on bulk lattice thermal conductivity, an argument that is supported by the fact the lattice contribution to the heat capacity, as well as the Debye temperature of these materials, is virtually unchanged by such a substitution. Previous studies of half-Heusler alloys support this claim, reporting little change in lattice thermal conductivity accompanying levels of transition-metal doping of the order of a few percent.[32,33]

V. CONCLUSIONS

The substitution of small concentrations of vanadium to the lower-valent transition-metal site of $Hf_{0.75}Zr_{0.25}NiSn$ has been shown to enhance the Seebeck coefficient of that compound over a broad range of temperatures in excess of 300 K while producing little effect on the electrical resistivity. The consequent enhancement in the thermoelectric power factor persists from room temperature to 650 K before the chemical potential begins to reach beyond the gap region and therefore away from the local resonance in the density of states. Hall measurements, calculations of effective mass, and heat capacity measurements indicate that this augmentation stems from the near doubling of the density of states near the Fermi energy from 2.2 to 4.0 states/eV per unit cell. This enhancement, however, persists over an energy scale only of the order of 50 meV, which is consistent with the introduction of resonant vanadium-induced states that are situated within the gap region, a phenomenon widely reported in II-VI and III-V semiconductors but heretofore not seen in half-Heusler materials. The results reported in this paper therefore imply a greater generality of the formation of resonant states through chemical substitution than had been previously expected.

In this light, it is no surprise that incrementing the number of *n*-type carriers through the typical method of Sb doping produces much the same effect via band filling. While it is therefore unlikely that small amounts of vanadium substitution will lead to increased *ZT* in half-Heusler compounds, an investigation of the possibility of introducing a resonance deeper into the conduction band could indeed prove promising. Resonant states in general are known to be highly sensitive to the effects of impurity valence and electronegativity, and those resonances induced by other transition-metal dopants may be more successful at enhancing the thermoelectric properties of half-Heusler and other thermoelectric alloys at high temperatures.

ACKNOWLEDGMENTS

The authors wish to thank M. Commisso for her assistance with the Hall measurements and to A. Cheung for assistance with the EDS measurements. The work at Clemson University is supported by DOE/EPSCoR Implementation Grant (No. DE-FG02-04ER-46139), and the SC EPSCoR cost-sharing program.

*Corresponding author: jsimonson@bnl.gov

[1]G. D. Mahan and J. O. Sofo, Proc. Natl. Acad. Sci. **93**, 7436 (1996).

[2]D. Bilc, S. D. Mahanti, E. Quarez, K.-F. Hsu, R. Pcionek, and M. G. Kanatzidis, Phys. Rev. Lett. **93**, 146403 (2004).

[3]S. Ahmad, K. Hoang, and S. D. Mahanti, Phys. Rev. Lett. **96**, 056403 (2006).
[4]J. P. Heremans, V. Jovovic, E. S. Toberer, A. Saramat, K. Kurasaki, A. Charoenphakdee, S. Yamanaka, and G. J. Snyder, Science **321**, 554 (2008).
[5]J.-H. Lee, J. Wu, and J. C. Grossman, Phys. Rev. Lett. **104**, 016602 (2010).
[6]J. Wu, W. Shan, and W. Walukiewicz, Semicond. Sci. Technol. **17**, 860 (2002).
[7]B. R. K. Nanda and I. Dasgupta, J. Phys. Cond. Matt. **17**, 5037 (2005).
[8]V. A. Romaka, M. G. Shelyapina, Y. K. Gorelenko, D. Fruchart, Y. V. Stadnyk, L. P. Romaka, and V. F. Chekurin, Semiconductors **40**, 655 (2006).
[9]J. W. Simonson and S. J. Poon, J. Phys. Cond. Matt. **20**, 255220 (2008).
[10]S. D. Mahanti, P. Larson, D. Y. Chung, S. Sportouch, and M. G. Kanatzidis, Mater. Res. Soc. Symp. Proc. **545**, 23 (1999).
[11]T. Stopa, J. Tobola, S. Kaprzyk, E. K. Hill, and D. Fruchart, J. Phys. Cond. Matt. **18**, 6379 (2006).
[12]H. Muta, T. Kanemitsu, K. Kurosaki, and S. Yamanaka, in *Proceedings of the 25th International Conference on Thermoelectrics* (IEEE, Piscataway, NJ, 2006), pp. 120–123.
[13]P. Qiu, X. Huang, X. Chen, and L. Chen, J. Appl. Phys. **106**, 103703 (2009).
[14]P. Qiu, J. Yang, X. Huang, X. Chen, and L. Chen, Appl. Phys. Lett. **96**, 152105 (2010).
[15]D. Bilc and P. Ghosez, e-print arXiv:1102.3346v1.
[16]A. C. Larson and R. B. Von Dreele, Los Alamos National Laboratory Report No. LAUR 86-748 (2000).
[17]B. H. Toby, J. Appl. Cryst. **34**, 210 (2001).
[18]S. R. Culp, S. J. Poon, N. Hickman, T. M. Tritt, and J. Blumm, Appl. Phys. Lett. **88**, 042106 (2006).
[19]V. I. Fistul, *Heavily Doped Semiconductors* (Plenum, New York, 1969).
[20]G. H. Jonker, Philips Res. Rep. **23**, 131 (1968).
[21]T. Sekimoto, K. Kurosaki, H. Muta, and S. Yamanaka, J. Appl. Phys. **99**, 103701 (2006).
[22]G. S. Nolas, J. Yang, and H. J. Goldsmid, *Thermal Conductivity: Theory, Properties, and Applications* (Plenum, New York, 2004), and references therein.
[23]F. G. Aliev, N. B. Brandt, V. V. Moshchalkov, V. V. Kozyrkov, R. V. Skolozdra, and A. I. Belogorokhov, Z. Phys. B Cond. Matt. **75**, 167 (1989).
[24]C. S. Lent, M. A. Bowen, R. S. Allgaier, J. D. Dow, O. F. Sankey, and E. S. Ho, Solid State. Commun. **61**, 83 (1987).
[25]S.-W. Kim, Y. Kimura, and Y. Mishima, Intermetallics **15**, 349 (2007).
[26]A. F. Ioffe, *Semiconductor Thermoelectrics and Thermoelectric Cooling* (Infosearch, London, 1957).
[27]M. Cutler and N. F. Mott, Phys. Rev. **181**, 1336 (1969).
[28]J. Mycielski, Solid State Commun. **60**, 165 (1986).
[29]Z. Wilamowski, K. Swiatek, T. Dietl, and J. Kossut, Solid state Commun. **74**, 833 (1990).
[30]F. G. Aliev, Physica B **171**, 199 (1991).
[31]S. R. Culp, J. W. Simonson, S. J. Poon, V. Ponnambalam, J. Edwards, and T. M. Tritt, Appl. Phys. Lett. **93**, 022105 (2008).
[32]T. J. Zhu, K. Xiao, C. Yu, J. J. Shen, S. H. Yang, A. J. Zhou, X. B. Zhao, and J. He, J. Appl. Phys. **108**, 044903 (2010).
[33]T. Wu, W. Jiang, X. Li, Y. Zhou, and L. Chen, J. Appl. Phys., **102**, 103705 (2007).